ACS central science

Research Article

Cite This: ACS Cent. Sci. 2019, 5, 1507−1513

http://pubs.acs.org/journal/acscii

Characterization of Reactive Organometallic Species via MicroED

Christopher G. Jones,[†,$] Matthew Asay,[†,$] Lee Joon Kim,[†] Jack F. Kleinsasser,[#] Ambarneil Saha,[†,‡] Tyler J. Fulton,[§] Kevin R. Berkley,[#] Duilio Cascio,[†,‡] Andrey G. Malyutin,[+] Matthew P. Conley,[#] Brian M. Stoltz,*[,§] Vincent Lavallo,*[,#] José A. Rodríguez,*[,†,‡] and Hosea M. Nelson*[,†]

[†]Department of Chemistry and Biochemistry and [‡]UCLA-DOE Institute for Genomics & Proteomics, University of California, Los Angeles, California 90095, United States

[#]Department of Chemistry, University of California, Riverside, California 92521, United States

[§]The Warren and Katharine Schlinger Laboratory for Chemistry and Chemical Engineering, Division of Chemistry and Chemical Engineering and [+]Beckman Institute, California Institute of Technology, Pasadena, California 91125, United States

Supporting Information

ABSTRACT: Here we apply microcrystal electron diffraction (MicroED) to the structural determination of transition-metal complexes. We find that the simultaneous use of 300 keV electrons, very low electron doses, and an ultrasensitive camera allows for the collection of data without cryogenic cooling of the stage. This technique reveals the first crystal structures of the classic zirconocene hydride, colloquially known as "Schwartz's reagent", a novel Pd(II) complex not amenable to solution-state NMR or X-ray crystallography, and five other paramagnetic and diamagnetic transition-metal complexes.

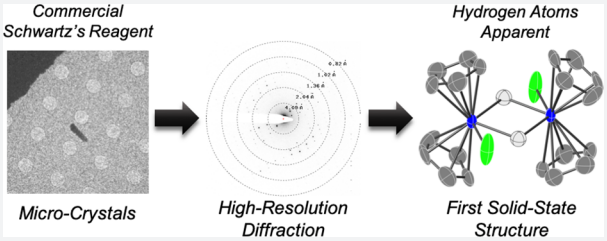

INTRODUCTION

For over a century, crystallography has fueled developments in modern chemistry. Within the chemical enterprise, crystallography has played a particularly special role in organometallic chemistry. Here, NMR-silent nuclei, paramagnetic spin, diversity of bonding and coordination environments, and poor reactivity profiles hinder the application of many solution-state characterization techniques. However, the need for carefully prepared single crystals with dimensions on the order of 0.1 mm^3 can also limit the application of X-ray crystallography. Moreover, neutron diffraction can be limited by the requirement of even larger crystals (~0.5 mm^3) and incompatibility with boron-containing compounds, as a result of destructive nuclear reactions.[1] Electron diffraction, as opposed to X-ray diffraction, offers several benefits, primarily the ability to circumvent the need for such large crystals for successful structural analysis of molecular compounds. Since earlier work by Kolb et al.[2] and Mugnaioli et al.[3] to adapt 3D electron diffraction techniques for structural analysis, several studies using a variety of electron diffraction techniques have been employed to structurally characterize inorganic and organic−inorganic hybrid materials such as metal organic frameworks.[4−10] Although these studies demonstrate the power of such techniques, we aim to adapt this method as a routine structural characterization tool for inorganic and organometallic chemists who often rely on traditional X-ray analysis as their primary means of characterization for highly reactive and unstable compounds. Here we employ the electron diffraction technique MicroED under ambient temperature using a 300 keV TEM to structurally characterize several organometallic compounds, reactive intermediates, and transition-metal coordination complexes, which are of interest to the practicing chemist and are often employed as catalytic reagents for a variety of important synthetic transformations. Despite there being several different methods for the collection of electron diffraction data, we found that the continuous-rotation technique used for MicroED is readily implemented on currently available instruments, and data obtained from this method is easily processed using standard, freely available, crystallographic software.[11] The MicroED method itself, which has typically been employed for large macromolecular structure analysis, is often performed under cryogenic conditions to preserve the hydration state of such biomolecules. However, prior studies have shown that by leveraging sensitive detectors, it is possible to use low electron doses to collect diffraction for small molecule structure determination under ambient temperatures, even for compounds that are particularly beam sensitive.[12−15] Using ambient temperature MicroED, we successfully resolve the first crystal structure of the privileged hydrozirconation reagent chloridobis(η^5-cyclopentadienyl)hydridozirconium, colloquially known as Schwartz's reagent, which was obtained from bulk powder utilized as purchased and determined by direct methods. We also report an ab initio structure of a Pd(II) 1,2-dipallidated alkyl species, obtained as a precipitant from the reaction mixture of ethylene with a pseudo-low-coordinate Pd(I) dimer. As a demonstration of the broad applicability of MicroED, we

Received: April 19, 2019
Published: September 6, 2019

DOI: 10.1021/acscentsci.9b00403
ACS Cent. Sci. 2019, 5, 1507−1513

also determine the structures of five other transition-metal complexes.

RESULTS AND DISCUSSION

Having recently reported the application of the CryoEM method MicroED to determine structures of several complex organic molecules,[16] we now evaluated the facility with which MicroED could interrogate complex organometallic species. We were particularly interested in chemical entities that failed to yield structures by conventional structural elucidation methods—crystallography or solution-state characterization. We first interrogated the structure of chloridobis(η^5-cyclopentadienyl)hydridozirconium **1** (Figure 1A),[17] a well-known industrial catalyst colloquially referred to as Schwartz's reagent. Schwartz's reagent sees widespread use in modern organic synthesis and is useful for a number of unique transformations mediated via hydrozirconation intermediates.[18−20] However, despite its synthetic relevance and the countervailing fact that half a century has transpired since Wailes and Weigold first discovered this species,[21,22] no single crystal structure of this canonical zirconocene complex has been obtained. This gap in crystallographic data has been attributed to the low solubility of the complex in hydrocarbon and ethereal solvents and its reactivity with polar chlorinated solvents,[23] precluding its crystallization and hindering NMR studies. As such, the currently accepted structure of Schwartz's reagent, a centrosymmetric dimer doubly linked by two bridging hydride ligands, represents a reconstruction from a combination of FTIR spectroscopy,[21,22] solid-state ^{35}Cl NMR studies,[24] and X-ray diffraction of related complexes.[25] To confirm this inferred structure, we subjected commercially acquired Schwartz's reagent to ambient temperature MicroED. Continuous-rotation data was collected from three crystals (Movie S1) at ambient temperature (ca. 23 °C), using a low-flux 300 keV electron beam (e.g., below 0.01 $e^-/Å^2$ per second) and a TVIPS XF-416 camera in rolling shutter mode (Figure 3B). The resulting diffraction was reduced and merged to obtain a high-completeness (90.6%) data set resolved at 1.15 Å. The room temperature Schwartz's structure was then determined ab initio by direct methods and refined to reveal the expected centrosymmetric dimer. Importantly, refinement proceeded smoothly and required no ex post facto corrections, calculations, or molecular replacement procedures.[26] The structure with riding hydrogens on the cyclopentadienyl ligands refined with anisotropic displacement parameters to an R_1 value of 14.9%. Critically, we had already observed suggestive regions of electron density consistent with bridging hydrides in the initial difference Fourier map (Figure 1B). To trace this more explicitly, we tracked peaks in the screened Coulomb potential within the unit cell, representing atomic locations. A sampling of consecutive two-dimensional slices in real space along the *a*-axis at the central mirror plane, which runs orthogonal to the cyclopentadienyl rings but bisects the zirconium, chlorine, and hydrogen atoms (Figure 1C and Movie S2) shows two hydrides emerging from the void space of the noise floor, thus corroborating the hydride positions observed during structural refinement (Figure 1D).

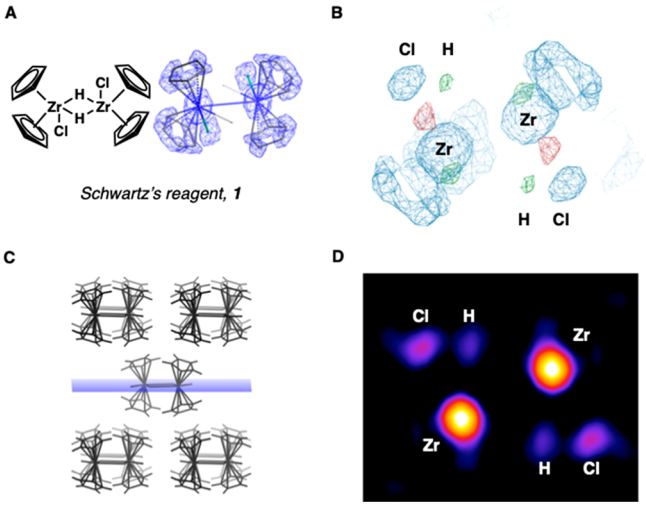

Figure 1. (A) Proposed structure of Schwartz's reagent and the refined structure with potential map overlay (R_1 = 14.9%, GooF = 2.254, completeness = 90.6%, resolution = 1.15 Å). (B) Prerefinement difference Fourier map generated using default X-ray scattering factors. Isolated green lobes indicate diagnostic regions of electron density geometrically consistent with doubly bridging hydrides. (C) Unit cell of the refined crystal structure generated by applying electron scattering parameters, viewed at a slight tilt along the a-axis. Highlighted slice in dark blue corresponds to the (0 0 2) Bragg plane. (D) Contour map of the central mirror plane depicted in (C) with the screened Coulomb potential of hydrides clearly visible.

Concurrent to our study of the application of MicroED to organometallic species, we sought to apply this powerful technique to active research problems in our groups including the reactivity of dimeric Pd(I) complexes. Dimeric palladium(I) species featuring Pd−Pd bonds have been previously reported to react with a variety of small molecules to give homolytic cleavage[27] or insertion products.[28] Pd(I) dimer **2** (Figure 2), synthesized by thermolysis or UV irradiation of the methyl palladium phosphine precursor,[29] was fully characterized by single crystal XRD (Figure 2B) and multinuclear NMR (see Supporting Information). To study the reactivity of this species (**2**), a THF solution was treated with ethylene gas, which interestingly led to a dramatic color change and precipitation of a yellow solid (Figure 2A). Efforts to characterize this solid, however, were frustrated by the lack of solubility and fragile nature of the putative ethylene adduct, as treatment of the precipitant with a variety of crystallization and/or NMR solvents led to rapid gas release and reformation of starting material **2**. Typically, such physical properties of a reactive intermediate would preclude definitive structural characterization. The yellow precipitate was instead taken directly from the reaction mix and deposited on an EM grid for characterization by MicroED. Remarkably, under high magnification, the apparently amorphous solid proved to have nanocrystalline domains that yielded the electron diffraction patterns shown in Figure S2. Diffraction movies were reduced to yield a high-completeness data set that produced an ab initio solution, which during refinement led to the definitive structural assignment of the species as the unexpected oxidative insertion product **3**. Such ethylene insertion products have been reported but remain rare.[30−32] This structure features two Pd(II) phosphine moieties linked by the reduced ethylene linker (Figure 2C, D). The extended linker precludes ipso-π-arene interactions of the phosphines, and therefore, one equivalent of THF completes the coordination sphere of each palladium center. The solid-state $^{13}C\{^1H\}$ cross-polarization magic angle spinning (CPMAS) NMR spectrum of **3** contains a signal at 37 ppm assigned to the reduced ethylene fragment (Figure S16). The $^{11}B\{^1H\}$ and

DOI: 10.1021/acscentsci.9b00403
ACS Cent. Sci. 2019, 5, 1507−1513

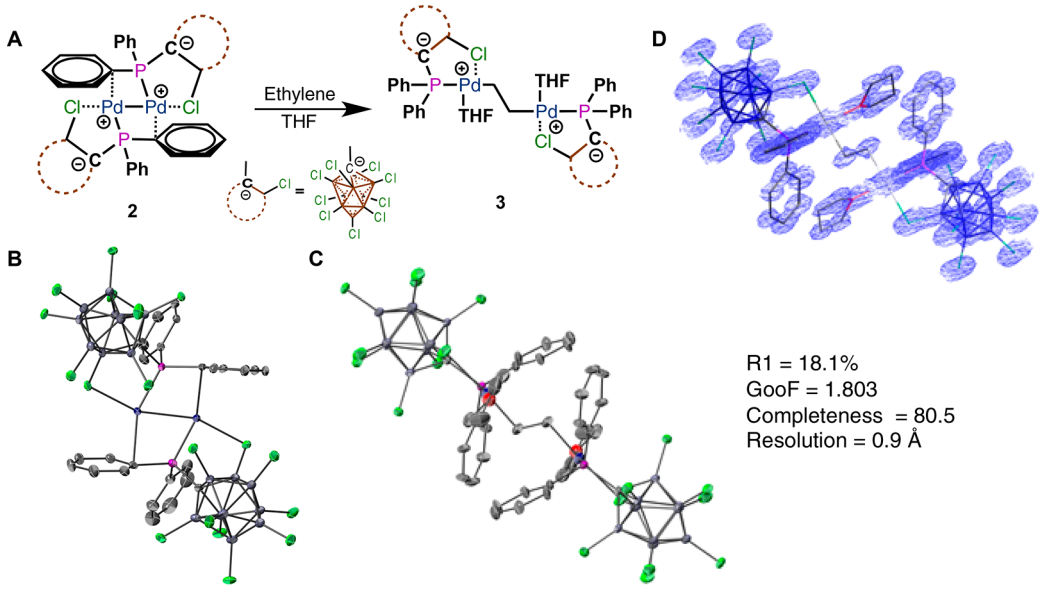

Figure 2. (A) Reaction of Pd(I) dimer **2** to form ethylene insertion product **3**. (B) X-ray crystal structure of complex **2**. (C) Ambient temperature electron diffraction structure of the ethylene insertion product **3**. (D) Coulomb potential map overlaid on the structure of **3**. (The hydrogen atoms and solvents of crystallization omitted for clarity).

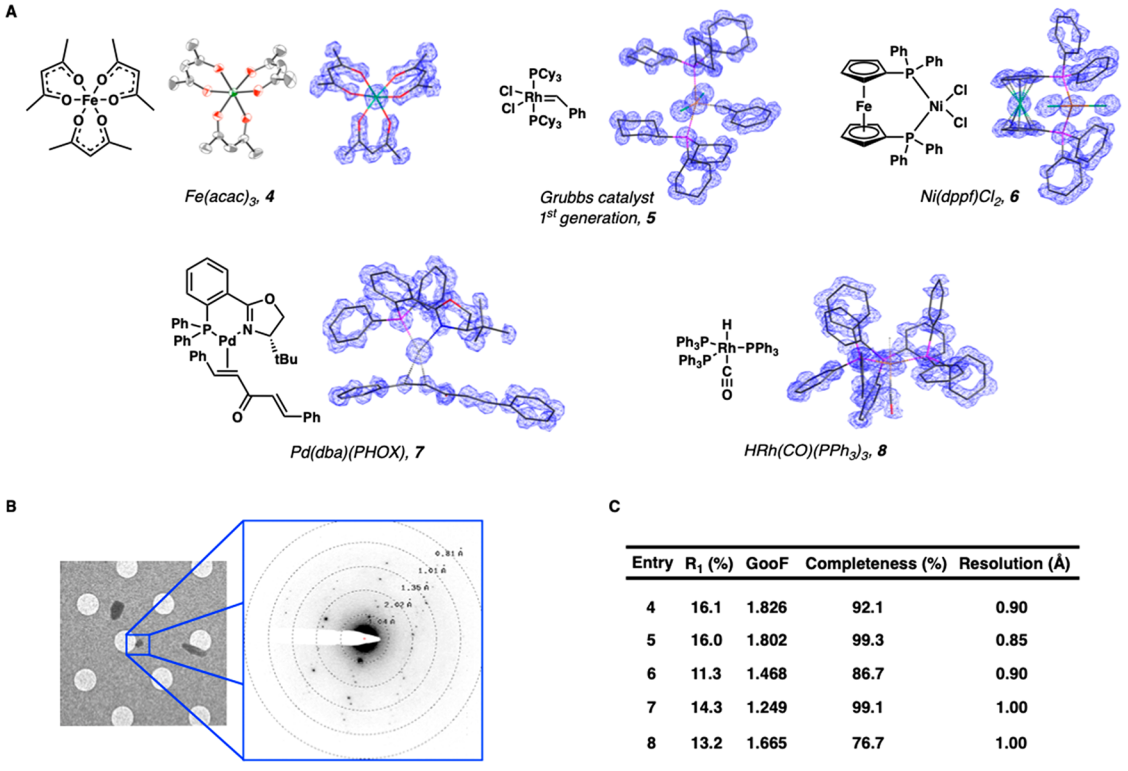

Entry	R_1 (%)	GooF	Completeness (%)	Resolution (Å)
4	16.1	1.826	92.1	0.90
5	16.0	1.802	99.3	0.85
6	11.3	1.468	86.7	0.90
7	14.3	1.249	99.1	1.00
8	13.2	1.665	76.7	1.00

Figure 3. Structures obtained by ambient temperature MicroED method. (A) Chemical structures and Coulomb potential maps of common-use transition-metal complexes. ORTEP diagram of $Fe(acac)_3$ is provided. For ORTEP diagrams of other organometallic compounds, see Figures S1–S7. (B) Example of an electron diffraction pattern obtained from submicron scale crystals. Grid holes are 1 μm in diameter. (C) Data and statistics obtained by ambient temperature MicroED.

$^{31}P\{^1H\}$ CPMAS NMR spectroscopy (Figures S17 and S18) are also consistent with the structure of **3** obtained from microED measurements. These NMR spectra also demonstrate the homogeneity of the sample.

To establish the generality of our approach we went on to determine structures of five additional commonly used organometallic compounds and transition-metal coordination complexes (Figure 3). The structures of tris(acetylacetonato)-iron(III) [$Fe(acac)_3$] (**4**), benzylidene-bis-(tricyclohexylphosphino)-dichlororuthenium (Grubbs' first generation catalyst) (**5**), [1,1-bis(diphenylphosphino)-ferrocene]dichloronickel(II) (**6**), Pd(dibenzylideneacetone)-((*S*)-4-*tert*-butyl-2-[2-(diphenylphosphino)phenyl]-2-oxazoline) (Pd(dba)(PHOX)) (**7**), and carbonyl(hydrido)tris-

DOI: 10.1021/acscentsci.9b00403
ACS Cent. Sci. 2019, 5, 1507–1513

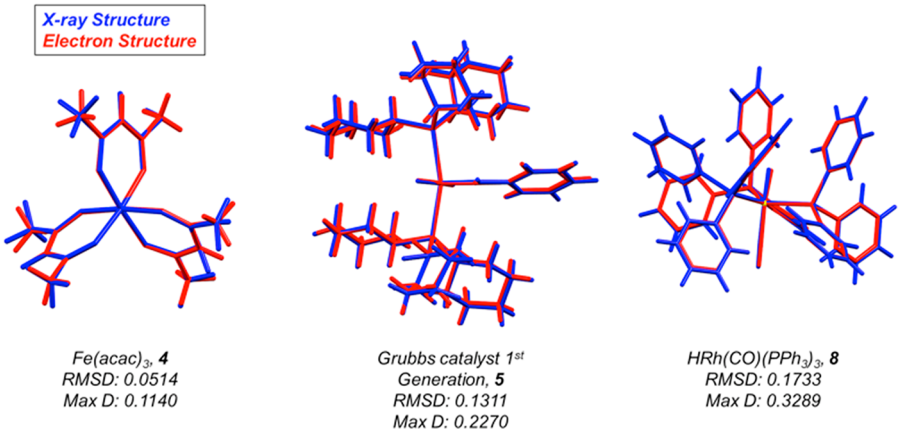

Figure 4. Overlay of ambient temperature ED (red) and previously reported X-ray diffraction (blue) structures for compounds **4**, **5**, and **8** with calculated root-mean-square deviation (Å) and maximum deviation (Å) of atomic coordinates.

(triphenylphosphane)rhodium(I) [$HRh(CO)(PPh_3)_3$] (**8**), (Figure 3A), were all determined using direct methods from data collected at noncryogenic temperatures. Together, this set of molecular structures demonstrates the utility of ambient temperature electron diffraction for the study of transition-metal complexes. Bulk powders of these compounds were analyzed by MicroED as described above, and data collected from one or more crystals were merged resulting in the assignment of space group and unit cell parameters that closely matched published values for XRD structures of these compounds, with the exception of compounds **6** and **7**, which are new polymorphs.[33,36] For a direct comparison, electron diffraction structures of compounds **4**, **5**, and **8** were overlaid with previously reported X-ray structures.[37,39] Root-mean-square (RMS) values were calculated based on the deviation of atomic position resulting in RMS values of 0.0514, 0.1311, 0.1733 Å and a maximum deviation of 0.1140, 0.2270, and 0.3289 Å for compounds **4**, **5**, and **8**, respectively (Figure 4). On the basis of the overlaid structures, the position of the observed hydride in the case of the Rh−H complex (**5**) is both geometrically and symmetrically consistent with the published X-ray crystallographic data with a deviation of 0.164 Å.[40] Although the published structures of these compounds are associated with lower statistical errors in general, our ambient temperature MicroED structures were determined from bulk powders (i.e., no formal recrystallization) and maintain sufficiently accurate statistical parameters (Figure 3C) to unambiguously characterize the connectivity of these compounds. These considerations render electron diffraction a powerful alternative for structural determination of transition-metal hydride structures.

Several previous studies use electron diffraction data for the determination of hydrogen atom positions[41−44] in metal hydrides, which are capable of exhibiting different chemical, electronic, and bonding properties in comparison to typical hydrogen atoms, and thus, the current quality of electron diffraction data obtained in this study does not allow for their unambiguous placement with high-enough precision to facilitate accurate discussion of bond lengths and angles. Although collecting data in continuous-rotation mode helps reduce dynamical scattering, residual dynamical scattering present in the data limits the accuracy of refinements based on a kinematical scattering approximation, and therefore, bond distances derived in this way can potentially be chemically inconsistent.[45] This problem has been well-analyzed by several other groups including Palatinus et al., who have used dynamical refinement on electron diffraction data collected in precession mode to help reduce statistical errors in atomic placement and bonding.[43,45,46,47] It is expected that such statistics of hydride localization as well as bond lengths and angles for all atomic constituents will improve with subsequent amelioration of microscopes and detectors. Furthermore, improvements in refinement software such as Jana, which has previously been used for processing of precession data, may now allow the possibility of applying dynamical refinements to continuous-rotation data, further reducing statistical error.[42,43]

CONCLUSIONS

Ambient temperature electron diffraction is an advantageous step toward the routine determination of organometallic species and potentially applicable to a wide array of small molecule organometallic and inorganic solids. The ability to routinely solve structures from nanocrystalline material and unambiguously determine the position of all atoms, including historically challenging hydrides attached to heavy atoms, presents chemists with a potent tool for the broad identification and characterization of elusive, but relevant, complexes. Armed with this method, we have determined structures of a diverse series of organometallic compounds and transition-metal coordination complexes, including those obtained from both commercial and laboratory synthesis. Importantly, each of these structures was determined ab initio by direct methods and refined using methods common to XRD. Our application of ambient temperature MicroED to the structure determination of Schwartz's reagent, obtained directly from the commercial seemingly amorphous powder, highlights the power of this new approach. Despite the importance of this molecule in synthetic chemistry, no previous high-resolution crystal structures have been obtained, as a result of the seemingly amorphous nature of the white powder obtained by precipitation during its preparation. Our ambient temperature MicroED structure not only confirms the dimeric nature of the reagent but more remarkably identifies the likely locations of bridging hydrides that are visible in electrostatic potential maps and can be refined freely. This method also allows for the determination of an unusual Pd(II) intermediate that was not amenable to structure determination by solution-state NMR or single crystal X-ray diffraction. Moreover, neutron diffraction would be incompatible with this

DOI: 10.1021/acscentsci.9b00403
ACS Cent. Sci. 2019, 5, 1507−1513

compound because of destructive boron neutron capture nuclear reactions. Importantly, although several protein structures have been determined by MicroED using molecular replacement, and structures of small molecules and polypeptides of known connectivity have been determined from MicroED data via direct methods, the reported Pd(II) complex (**3**) is a rare example of a novel complex small molecule identified by MicroED without prior knowledge of the structure or other corroborating solution-state spectroscopic methods. Although our data does not facilitate extensive discussions of bond lengths or angles because of higher-than-expected statistical errors in refinement compared to traditional XRD, the fact that cryogenic temperatures are not required to obtain structural information from reactive metal complexes is ground-breaking, as many research institutions can make rapid use of readily available TEM facilities. Moreover, utilization of a more sensitive and faster detector, with shorter dead-time,[11] reduces peak overlap between frames as well. Ambient temperature measurements also dramatically simplify sample preparation and loading, eliminating issues typically associated with cryogenic cooling that often complicate crystal screening and data collection (e.g., ice deposition). We envision that microelectron diffraction will continue to improve and find new applications in the molecular sciences. Efforts directed toward a multitude of new frontiers in small molecule electron diffraction are already underway. These efforts are expected to bring new horizons for small molecule structure determination over the coming months and years.

■ ASSOCIATED CONTENT

Supporting Information

The Supporting Information is available free of charge on the ACS Publications website at DOI: 10.1021/acscentsci.9b00403.

Procedures, chemical suppliers, crystallographic data, and spectrographic data (PDF)
Continuous-rotation MicroED data (MP4)
Contour plot for Schwartz's reagent (MP4)
CCDC 1908168 = Compound 1 (CIF)
CCDC 1908169 = Compound 2 (CIF)
CCDC 1908170 = Compound 3 (CIF)
CCDC 1908171 = Compound 4 (CIF)
CCDC 1908172 = Compound 5 (CIF)
CCDC 1908173 = Compound 6 (CIF)
CCDC 1908174 = Compound 7 (CIF)
CCDC 1908175 = Compound 8 (CIF)

■ AUTHOR INFORMATION

Corresponding Authors

*E-mail: stoltz@caltech.edu. (B.M.S.)
*E-mail: vincent.lavallo@ucr.edu. (V.L.)
*E-mail: jrodriguez@mbi.ucla.edu. (J.A.R.)
*E-mail: hosea@chem.ucla.edu. (H.M.N.)

ORCID

Brian M. Stoltz: 0000-0001-9837-1528
Vincent Lavallo: 0000-0001-8945-3038
Hosea M. Nelson: 0000-0002-4666-2793

Author Contributions

$C.G.J. and M.A. contributed equally. C.G.J. performed experiments, developed the sample preparation techniques, processed and refined structural data, prepared figures, and assisted with manuscript preparation. M.A. prepared samples, refined structural data, and assisted with manuscript and figure preparation. L.J.K. performed experiments, processed structural data, prepared figures, and assisted with manuscript preparation. J.F.K. prepared isolated and characterized compounds. A.S. processed and refined data, wrote and executed MATLAB code, prepared figures, and assisted in manuscript preparation. T.J.F. performed experiments and assisted with manuscript preparation. K.R.B. prepared isolated and characterized compounds. D.C. assisted in processing and refining structural data and provided crystallographic expertise. A.G.M. assisted in data collection. M.P.C. performed solid-state NMR experiments. B.M.S. designed experiments and assisted with manuscript preparation. V.L. designed experiments and assisted with manuscript preparation. J.A.R. performed experiments, developed sample preparation techniques, maintained the microscope, analyzed data, and assisted with manuscript preparation. H.M.N. conceived of the project, designed experiments, performed experiments, developed the sample preparation techniques, and assisted with manuscript and figure preparation.

Notes

The authors declare no competing financial interest.

■ ACKNOWLEDGMENTS

The authors thank Michael R. Sawaya, Michael K. Takase, Michael J. Collazo, Marcus Gallagher-Jones, and Chih-Te Zee (University of California, Los Angeles) for technical expertise and inspirational discussions. This material is based upon work supported by the National Science Foundation Graduate Research Fellowship (to C.G.J. and A.S.) under Grant No. DGE-1650604. This work is funded by STROBE, an NSF STC under Grant No. DMR 1548924. This work was supported by the University of California, Riverside. The solid-state NMR measurements at 14.1 T were recorded on an instrument supported by the National Science Foundation (CHE-1626673). V.L. acknowledges support from the National Science Foundation (CHE-1455348). J.A.R. acknowledges support from the Arnold and Mabel Beckman Foundation, the Pew Charitable Trusts, the Searle Scholars Program, the U.S. Department of Energy (Grant No. DE-FC02-02ER63421), and the National Institutes of Health—National Institute of General Medical Sciences (Grant Nos. P41 GM102403 and R35 GM128867). H.M.N. acknowledges support from the David and Lucile Packard Foundation, the Alfred P. Sloan Foundation, and the Pew Charitable Trusts. The authors thank the Beckman Institute Resource Center for Transmission Electron Microscopy at Caltech.

■ REFERENCES

(1) Nedunchezhian, K.; Aswath, N.; Thiruppathy, M.; Thirugnanamurthy, S. Boron neutron capture therapy - A literature review. *J. Clin. Diagn. Res.* **2016**, *10*, ZE01−ZE04.
(2) Kolb, U.; Gorelik, T.; Kübel, C.; Otten, M. T.; Hubert, D. Towards automated diffraction tomography: Part I—Data acquisition. *Ultramicroscopy* **2007**, *107*, 507−513.
(3) Mugnaioli, E.; Gorelik, T.; Kolb, U. "Ab initio" structure solution from electron diffraction data obtained by a combination of automated diffraction tomography and precession technique. *Ultramicroscopy* **2009**, *109*, 758−765.
(4) Portolés-Gil, N.; Lanza, A.; Aliaga-Alcalde, N.; Ayllón, J. A.; Gemmi, M.; Mugnaioli, E.; López-Periago, A. M.; Domingo, C.

DOI: 10.1021/acscentsci.9b00403
ACS Cent. Sci. 2019, 5, 1507−1513

Crystalline curcumin bioMOF obtained by precipitation in supercritical CO_2 and structural determination by electron diffraction tomography. *ACS Sustainable Chem. Eng.* **2018**, *6*, 12309−12319.
(5) Yuan, S.; Qin, J.-S.; Xu, H.-Q.; Su, J.; Rossi, D.; Chen, Y.; Zhang, L.; Lollar, C.; Wang, Q.; Jiang, H.-L.; Son, D. H.; Xu, H.; Huang, Z.; Zou, X.; Zhou, H.-C. $[Ti_8Zr_2O_{12}(COO)_{16}]$ cluster: An ideal inorganic building unit for photoactive metal−organic frameworks. *ACS Cent. Sci.* **2018**, *4*, 105−111.
(6) Denysenko, D.; Grzywa, M.; Tonigold, M.; Streppel, B.; Krkljus, I.; Hirscher, M.; Mugnaioli, E.; Kolb, U.; Hanss, J.; Volkmer, D. Elucidating gating effects for hydrogen sorption in MFU-4-type triazolate-based metal−organic frameworks featuring different pore sizes. *Chem. - Eur. J.* **2011**, *17*, 1837−1848.
(7) Feyand, M.; Mugnaioli, E.; Vermoortele, F.; Bueken, B.; Dieterich, J. M.; Reimer, T.; Kolb, U.; de Vos, D.; Stock, N. Automated diffraction tomography for the structure elucidation of twinned, sub-micrometer crystals of a highly porous, catalytically active bismuth metal−organic framework. *Angew. Chem., Int. Ed.* **2012**, *51*, 10373−10376.
(8) Wang, B.; Rhauderwiek, T.; Inge, A. K.; Xu, H.; Yang, T.; Huang, Z.; Stock, N.; Zou, X. A porous cobalt tetraphosphonate metal−organic framework: Accurate structure and guest molecule location determined by continuous-rotation electron diffraction. *Chem. - Eur. J.* **2018**, *24*, 17429−17433.
(9) Bellussi, G.; Montanari, E.; Di Paola, E.; Millini, R.; Carati, A.; Rizzo, C.; O'Neil Parker, W., Jr.; Gemmi, M.; Mugnaioli, E.; Kolb, U.; Zanardi, S. ECS-3: A crystalline hybrid organic−inorganic aluminosilicate with open porosity. *Angew. Chem., Int. Ed.* **2012**, *51*, 666−669.
(10) Yun, Y.; Zou, X.; Hovmoller, S.; Wan, W. Three-dimensional electron diffraction as a complementary technique to powder X-ray diffraction for phase identification and structure solution of powders. *IUCrJ* **2015**, *2*, 267−282.
(11) Gemmi, M.; La Placa, M. G. I.; Galanis, A. S.; Rauch, E. F.; Nicolopoulos, S. Fast electron diffraction tomography. *J. Appl. Crystallogr.* **2015**, *48*, 718−727.
(12) Gorelik, T. E.; van de Streek, J.; Kilbinger, A. F. M.; Brunklaus, G.; Kolb, U. Ab-initio crystal structure analysis and refinement approaches of oligo p-benzamides based on electron diffraction data. *Acta Crystallogr., Sect. B: Struct. Sci.* **2012**, *68*, 171−181.
(13) van Genderen, E.; Clabbers, M. T. B.; Das, P. P.; Stewart, A.; Nederlof, I.; Barentsen, K. C.; Portillo, Q.; Pannu, N. S.; Nicolopoulos, S.; Gruene, T.; Abrahams, J. P. Ab initio structure determination of nanocrystals of organic pharmaceutical compounds by electron diffraction at room temperature using a Timepix quantum area direct electron detector. *Acta Crystallogr., Sect. A: Found. Adv.* **2016**, *72*, 236−242.
(14) Das, P. P.; Mugnaioli, E.; Nicolopoulos, S.; Tossi, C.; Gemmi, M.; Galanis, A.; Borodi, G.; Pop, M. M. Crystal structures of two important pharmaceuticals solved by 3D precession electron diffraction tomography. *Org. Process Res. Dev.* **2018**, *22*, 1365−1372.
(15) Das, P. P.; Mugnaioli, E.; Nicolopoulos, S.; Tossi, C.; Gemmi, M.; Galanis, A.; Borodi, G.; Pop, M. M. Crystal structures of two important pharmaceuticals solved by 3D precession electron diffraction tomography. *Org. Process Res. Dev.* **2018**, *22*, 1365−1372.
(16) Jones, C. G.; Martynowycz, M. W.; Hattne, J.; Fulton, T. J.; Stoltz, B. M.; Rodriguez, J. A.; Nelson, H. M.; Gonen, T. The cryoEM method microED as a powerful tool for small molecule structure determination. *ACS Cent. Sci.* **2018**, *4*, 1587−1592.
(17) Hart, D. W.; Schwartz, J. Hydrozirconation. Organic synthesis via organozirconium intermediates. Synthesis and rearrangement of alkylzirconium(IV) complexes and their reaction with electrophiles. *J. Am. Chem. Soc.* **1974**, *96*, 8115−8116.
(18) Schwartz, J.; Labinger, J. A. Hydrozirconation: A new transition metal reagent for organic synthesis. *Angew. Chem., Int. Ed. Engl.* **1976**, *15*, 333−340.
(19) Wieclaw, M. M.; Stecko, S. Hydrozirconation of C = X functionalities with Schwartz's reagent. *Eur. J. Org. Chem.* **2018**, *2018*, 6601−6623.
(20) Pinheiro, D. L. J.; de Castro, P. P.; Amarante, G. W. Recent developments and synthetic applications of nucleophilic zirconocene complexes from Schwartz's reagent. *Eur. J. Org. Chem.* **2018**, *2018*, 4828−4844.
(21) Kautzner, B.; Wailes, P. C.; Weigold, H. Hydrides of bis(cyclopentadienyl)zirconium. *J. Chem. Soc. D* **1969**, 1105a.
(22) Wailes, P. C.; Weigold, H. Hydrido complexes of zirconium I. Preparation. *J. Organomet. Chem.* **1970**, *24*, 405−411.
(23) Takahashi, T.; Suzuki, N.; Jayasuriya, N.; Wipf, P. Chlorobis-(cyclopentadienyl)hydridozirconium. *Encyclopedia of Reagents for Organic Synthesis* **2006**.
(24) Rossini, A. J.; Mills, R. W.; Briscoe, G. A.; Norton, E. L.; Geier, S. J.; Hung, I.; Zheng, S.; Autschbach, J.; Schurko, R. W. Solid-state chlorine NMR of group IV transition metal organometallic complexes. *J. Am. Chem. Soc.* **2009**, *131*, 3317−3330.
(25) Harlan, C. J.; Bott, S. G.; Barron, A. R. Methyl−hydride metathesis between $[Zr(cp)_2Me_2]$ and $[HAl(\mu_3\text{-}NBut)]_4$: molecular structures of $[Me_{1-x}HxAl(\mu_3\text{-}NBu^t)]4$ (x = 0, 0.78 or 1) and $[(cp)_2ZrMe(\mu\text{-}H)]_2$ (cp = η^5-C_5H_5). *J. Chem. Soc., Dalton Trans.* **1997**, 637−642.
(26) The appropriate electron scattering factors were used; see: Peng, L. M. Electron atomic scattering factors and scattering potentials of crystals. *Micron* **1999**, *30*, 625−648.
(27) Fafard, C. M.; Adhikari, D.; Foxman, B. M.; Mindiola, D. J.; Ozerov, O. V. Addition of ammonia, water, and dihydrogen across a single Pd−Pd bond. *J. Am. Chem. Soc.* **2007**, *129*, 10318−10319.
(28) Huacuja, R.; Graham, D. J.; Fafard, C. M.; Chen, C.-H.; Foxman, B. M.; Herbert, D. E.; Alliger, G.; Thomas, C. M.; Ozerov, O. V. Reactivity of a Pd(I)−Pd(I) dimer with O_2: monohapto Pd superoxide and dipalladiumperoxide in equilibrium. *J. Am. Chem. Soc.* **2011**, *133*, 3820−3823.
(29) Kleinsasser, J. F.; Reinhart, E. D.; Estrada, J.; Jordan, R. F.; Lavallo, V. Ethylene oligomerization and polymerization by palladium(II) methyl complexes supported by phosphines bearing a perchlorinated 10-vertex *closo*-carborane anion substituent. *Organometallics* **2018**, *37*, 4773−4783.
(30) Hetterscheid, D. G. H.; Kaiser, J.; Reijerse, E.; Peters, T. P. J.; Thewissen, S.; Blok, A. N. J.; Smits, J. M. M.; de Gelder, R.; de Bruin, B. IrII(ethene): Metal or carbon radical? *J. Am. Chem. Soc.* **2005**, *127*, 1895−1905.
(31) Van Voorhees, S. L.; Wayland, B. B. Formation of metallo hydride, formyl, and alkyl complexes of Rh(TMTAA). *Organometallics* **1987**, *6*, 204−206.
(32) Huacuja, R. Synthesis and reactivity of unusual palladium (II) complexes supported by a diarylamido/BIS(phosphine) PNP pincer ligand. Ph.D. Dissertation, Texas A&M University, 2014; available electronically from http://hdl.handle.net/1969.1/152457.
(33) Weng, S.-S.; Ke, C.-S.; Chen, F.-K.; Lyu, Y.-F.; Lin, G.-Y. Transesterification catalyzed by iron(III) β-diketonate species. *Tetrahedron* **2011**, *67*, 1640−1648.
(34) Torker, S.; Müller, A.; Sigrist, R.; Chen, P. Tuning the steric properties of a metathesis catalyst for copolymerization of norbornene and cyclooctene toward complete alternation. *Organometallics* **2010**, *29*, 2735−2751.
(35) Casellato, U.; Ajó, D.; Valle, G.; Corain, B.; Longato, B.; Graziani, R. Heteropolymetallic complexes of 1,1'-bis-(diphenylphosphino) ferrocene (dppf). II. Crystal structure of dppf and $NiCl_2$(dppf). *J. Crystallogr. Spectrosc. Res.* **1988**, *18*, 583−590.
(36) Sherden, N. H.; Behenna, D. C.; Virgil, S. C.; Stoltz, B. M. Unusual allylpalladium carboxylate complexes: identification of the resting state of catalytic enantioselective decarboxylative allylic alkylation reactions of ketones. *Angew. Chem., Int. Ed.* **2009**, *48*, 6840−6843.
(37) Trnka, T. M. Catalyst for olefin metathesis: ruthenium alkylidene complexes with phosphine and *N*-heterocyclic ligands. Ph.D. Dissertation, California Institute of Technology, Pasadena, CA, 2002.
(38) Iball, J.; Morgan, C. H. A refinement of the crystal structure of ferric acetylacetonate. *Acta Crystallogr.* **1967**, *23*, 239−244.

DOI: 10.1021/acscentsci.9b00403
ACS Cent. Sci. 2019, 5, 1507−1513

(39) La Placa, S. J.; Ibers, J. A. Crystal and molecular structure of tritriphenylphosphine rhodium carbonyl hydride. *Acta Crystallogr.* **1965**, *18*, 511−519.
(40) Babra, I. S.; Morley, L. S.; Nyburg, S. C.; Parkins, A. W. The crystal and molecular structure of a new polymorph of carbonylhydridotris(triphenylphosphine)rhodium(I) having a Rh-H stretching absorption at 2013 cm^{-1}. *J. Crystallogr. Spectrosc. Res.* **1993**, *23*, 997−1000.
(41) Mugnaioli, E.; Gemmi, M. Single-crystal analysis of nano-domains by electron diffraction tomography: mineralogy at the order-disorder borderline. *Z. Kristallogr. - Cryst. Mater.* **2018**, *233*, 163−178.
(42) Hynek, J.; Brázda, P.; Rohlíček, J.; Londesborough, M. G. S.; Demel, J. Phosphinic acid based linkers: Building blocks in metal−organic framework chemistry. *Angew. Chem.* **2018**, *130*, 5110−5113.
(43) Palatinus, L.; Brázda, P.; Boullay, P.; Perez, O.; Klementová, M.; Petit, S.; Eigner, V.; Zaarour, M.; Mintova, S. Hydrogen positions in single nanocrystals revealed by electron diffraction. *Science* **2017**, *355*, 166−169.
(44) Clabbers, M. T. B.; Gruene, T.; van Genderen, E.; Abrahams, J. P. Reducing dynamical electron scattering reveals hydrogen atoms. *Acta Crystallogr., Sect. A: Found. Adv.* **2019**, *75*, 82−93.
(45) Palatinus, L.; Jacob, D.; Cuvillier, P.; Klementova, M.; Sinkler, W.; Marks, L. D. Structure refinement from precession electron diffraction data. *Acta Crystallogr., Sect. A: Found. Crystallogr.* **2013**, *69*, 171−188.
(46) Palatinus, L.; Petricek, V.; Correa, C. A. Structure refinement using precession electron diffraction tomography and dynamical diffraction: theory and implementation. *Acta Crystallogr., Sect. A: Found. Adv.* **2015**, *71*, 235−244.
(47) Palatinus, L.; Correa, C. A.; Steciuk, G.; Jacob, D.; Roussel, P.; Boullay, P.; Klementova, M.; Gemmi, M.; Kopecek, J.; Domeneghetti, M. C.; Camara, F.; Petricek, V. Structure refinement using precession electron diffraction tomography and dynamical diffraction: tests on experimental data. *Acta Crystallogr., Sect. B: Struct. Sci., Cryst. Eng. Mater.* **2015**, *71*, 740−751.

DOI: 10.1021/acscentsci.9b00403
ACS Cent. Sci. 2019, 5, 1507−1513